www.czasopisma.pan.pl PAN POLSKA AKADEMIA NAUK www.journals.pan.pl

Arch. Metall. Mater. **65** (2020), 2, 879-884

DOI: 10.24425/amm.2020.132834

D. SZALBOT[1]*, J. A. BARTKOWSKA[1], K. FELIKSIK[1], M. BARA[1], M. CHRUNIK[2], M. ADAMCZYK-HABRAJSKA[1]

CORRELATION BETWEEN STRUCTURE, MICROSTRUCTURE AND DIELECTRIC PROPERTIES OF $Bi_7Fe_3Ti_3O_{21}$ CERAMICS OBTAINED IN DIFFERENT CONDITIONS

Multiferroic six-layer Aurivillius type $Bi_7Fe_3Ti_3O_{21}$ ceramics was obtained by conventional mixed oxides method. The final sintering process was taken in several different sintering times, which determined changes in properties of discussed ceramic material. The structure and dielectric properties of the material are reported. In order to examine the technological conditions on the crystal structure, XRD analysis was carried out. The microstructure, as well as the quantitative and qualitative analysis of the chemical composition were investigated by scanning electron microscope with an energy dispersion spectrometer. The main purpose of the paper is to present the effect of sintering time on the microstructure, crystallographic structure and dielectric properties of $Bi_7Fe_3Ti_3O_{21}$ ceramics.

Keywords: multiferroic materials, Aurivillius phases, $Bi_7Fe_3Ti_3O_{21}$, dielectric properties

1. Introduction

Nowadays, where scientists aim at device's miniaturization, it causes the increase of interests in finding new, functional materials. Multiferroic materials are their representative. The properties of it change very strongly under the impact of external influences. They combine ferroelectric, (ferro)magnetic and/or ferroelastic properties simultaneously [1-3]. An interesting group of the multiferroic materials is perovskite-like layered structures called Aurivillius phases. Due to their properties, these materials can be used for example in optical devices, ferroelectric memories, actuators, transducers or humidity sensors [4-8]. The general formula of compounds with Aurivillius-type structure is $(Bi_2O_2)^{2+}(A_{m-1}B_mO_{3m+1})^{2-}$, for the first time described by Aurivillius in 1949 [9]. The value m (integer or fractional), indicates the number of perovskite building blocks between two fluorite-like bismuth-oxygen layers $(Bi_2O_2)^{2+}$ [10]. The place of A position usually is taken by big cations like Bi^{3+}, Sr^{2+}, Dy^{3+}, $La^{3+}$and the B position is mostly occupied by smaller ions like for example Fe^{3+}, Ti^{4+} [11].

Authors, repeatedly indicate, that single-phase samples $Bi_{m+1}Fe_{m-3}Ti_3O_{3m+3}$ are very difficult to obtained by solid-phase chemical reactions. The reason for this is the multi-stage process of the formation of these compounds and the fact that the thermal stability of the materials in question is low [12]. Therefore, it is still desirable to find a suitable method to obtain this material. The literature reports different ways to obtain the Aurivillius compounds, such as preparing through a modified sol-gel citrate-complexation and precursor film route [13], using Pechini's method [14,15] or obtaining samples by traditional solid-state technique [16]. The choice of the method as well as technological conditions have significant impact on properties of ceramic materials.

The aim of this work was to study the dielectric properties of six-layered Aurivillius type $Bi_7Fe_3Ti_3O_{21}$ ceramics obtained in different sintering times. XRD analysis was conducted to study the crystal structure.

2. Experimental

2.1. Technology process

Stoichiometric amount of simple oxides Bi_2O_3 (Aldrich 99,9%), TiO_2 (Poch 99,9%), Fe_2O_3 (Sigma-Aldrich 99%) were weighted, preliminarily mixed in the mortar and then milled in the planetary ball mill for t = 24 h (in ethanol). After drying, powders were re-mixed in the mortar. The synthesis was carried out at T = 1123 K for t = 4 h. The next step was to crumble the powders in the mortar and to mill it in ethanol in the planetary

[1] UNIVERSITY OF SILESIA, FACULTY OF SCIENCE AND TECHNOLOGY, INSTITUTE OF MATERIALS ENGINEERING, 12, ŻYTNIA STR., 41-200 SOSNOWIEC, POLAND
[2] INSTITUTE OF APPLIED PHYSICS, MILITARY UNIVERSITY OF TECHNOLOGY, 2 GEN. SYLWESTRA KALISKIEGO STR., 00-908 WARSZAW, POLAND

* Correspondence author: diana.szalbot@us.edu.pl

ball mill for $t = 24$ h over. After drying and next re-milling in the mortar, pellets were pressed ($\phi = 10$ mm, $H = 1$ mm, 200 MPa). The samples were put and closed into crucibles. The sintering was carried out under the following conditions: $T = 1263$ K for the several sintering time $t_s = (4;8;12;16;24)$ h.

2.2. Investigations

The scanning electron microscope was used to observe the microstructure of the ceramic samples. To confirm a proper stoichiometry of obtained material the energy dispersion spectroscopy (EDS) technique was applied. The crystal structures of all discussed samples were investigated using BRUKER D8 Discover, equipped with a standard CuKα radiator ($\lambda_{Ka1} = 1.54056$ Å, $\lambda_{Ka2} = 1.54439$ Å, Siemens KFL CU2 K, working at 40 kV voltage and 40 mA current in operating mode). The radiator was equipped with a Göbel FGM2 mirror, allowing to perform the measurements under parallel beam conditions. The Bragg-Brentano diffraction geometry was applied [17]. The diffraction angle of 2θ range was set to 15-80° with a step of 0.015° and acquisition time of 2 s per step. All measurements were done at 298 K in the temperature-stabilized Anton Paar HTK 1200N chamber. For the data processing the Crystal Impact Match! application was used. For each diffraction pattern the λ_{Ka2} signal component was deconvoluted and removed, the background was subtracted and

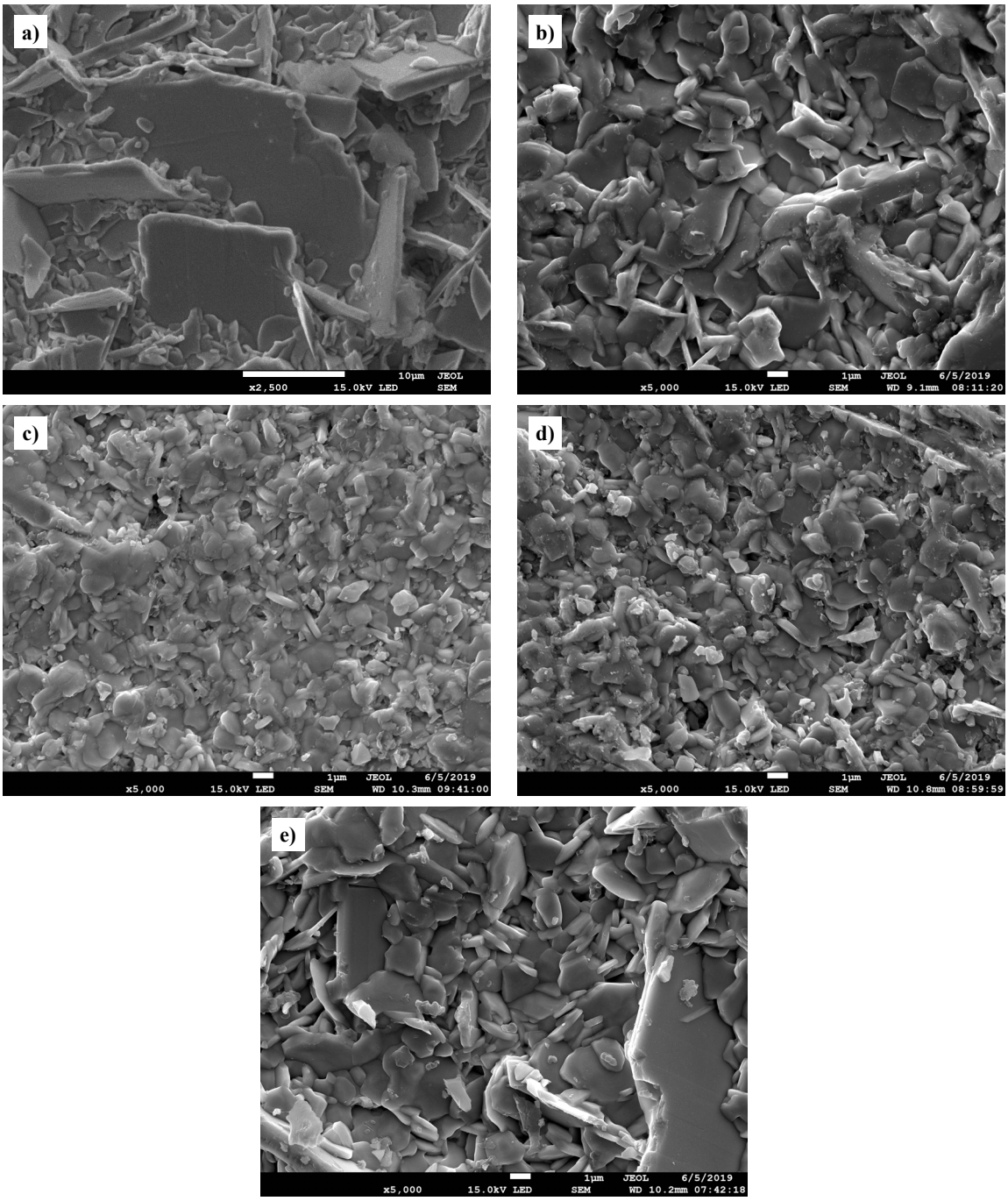

Fig. 1. SEM images of the microstructure of fracture of the $Bi_7Fe_3Ti_3O_{21}$ samples sintered from different time a) 4 h b) 8 h c) 12 h d) 16 h and e) 24 h

the data were smoothed using the fast Fourier transform. The phase analyzes were done with support of an ICSD database. For crystallographic calculations the FullPROF ver. 3.0 program was used, which allowed to perform the Rietveld refinement and calculate the precise unit cell parameters, based on a diffraction profile fitting [18]. The reference CIF file used for this analysis was received from the supplementary data given in Ref. [19]. Calculated broadening of diffraction lines, namely full width at half maximum (FWHM) was used to estimate the average crystallite sizes using Debye-Scherrer formula [20]. The standard reference material NIST SRM 660a (LaB_6) was applied as an instrumental standard to eliminate the apparatus broadening component.

The measurements of the temperature dependencies of dielectric permittivity were performed with the use a computerized measuring system, where the integral part was an Agilent E4980A LCR meter.

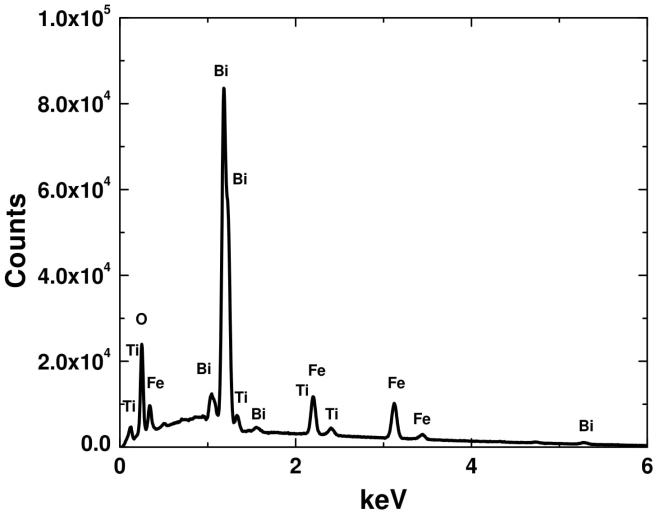

Fig. 2. EDS emission spectrum $Bi_7Fe_3Ti_3O_{21}$ ceramics sintered for $t = 4$ h

3. The results and discussion

Several different sintering times were applied at the final sintering process. The difference in technical conditions determined changes in properties of discussed ceramic material. Figure 1 exhibits SEM images of ceramic materials densified at different time. The grains of ceramics which were finally sintered for the shortest time are well developed and show platelet – like structure, which is characteristic for $Bi_{m+1}Fe_{m-3}Ti_3O_{3m+3}$ [21]. Such a shape is typical for Aurivillius bismuth layered compounds due to the preferential growth of the $a-b$ crystalline plain [22]. Plates are randomly oriented and their size is not homogenous, however the domination of larger grains is visible. The microstructure is completely changed as far as longer times of final sintering are concerned. The platelet-like grains completely disappeared, and much smaller grains with rounded edges developed. The tendency is changed for samples which were sintered for 24 hours.

The EDS spectrum is shown in Figure 2. The qualitative EDS analysis confirms the presence of following elements: bismuth, iron, titanium and oxygen. The presence of undesirable impurities has not been registered. The scan has been done on 50 points of several grains – the stoichiometry changes slightly from "point to point". However, the average stoichiometry obtained for the surface of all grains is in a good agreement with theoretical one. The Table 1 presents results of EDS analysis concerning $Bi_7Fe_3Ti_3O_{21}$ ceramics sintered for 4 h. The oxides content determined from EDS method for other discussed ceramics is similar.

The influence of sintering time length on the crystal structure of $Bi_7Fe_3Ti_3O_{21}$ ceramics has been studied by XRD. The complete set of the powder diffraction patterns with the reference ICSD card for investigated samples are shown in Figure 3. The unit cell parameters and estimated crystallite sizes were presented in Table 2.

The comparison of obtained results has shown that the increase of sintering time insignificantly influence on the crystallographic parameters, which has had tendency to decrease with increase in t_s. The effect of technological conditions on

TABLE 1

Theoretical and experimental content of elements (calculation for simple oxides) for $Bi_7Fe_3Ti_3O_{21}$ sintered for 4 h

$Bi_7Fe_3Ti_3O_{21}$ t_s = 4h			
Oxide formula	**Determined oxide content from EDS [wt.%]**	**Theoretical oxide content [wt.%]**	**The difference between the teoretical and determined oxide content [wt.%]**
Bi_2O_3	76.7	77.3	0.6
Fe_2O_3	12.6	11.4	1.2
TiO_2	10.8	11.4	0.6

TABLE 2

Unit cell parameters of as-prepared $Bi_7Fe_3Ti_3O_{21}$ samples along with their average crystallite sizes

Sintering time [h]	**Unit cell parameters [Å]**			**V [Å^3]**	**Crystallite size [nm]**
	a	**b**	**c**		
4	5.492(6)	5.540(1)	57.724(3)	1756.52	58
8	5.477(1)	5.490(1)	57.493(5)	1728.74	56
12	5.482(1)	5.491(1)	57.396(3)	1727.72	48
16	5.482(1)	5.492(1)	57.361(3)	1726.98	35
24	5.477(5)	5.497(5)	57.383(4)	1727.63	40
Ref. [19]	5.4699	5.4924	57.5510	1729.00	—

the change in crystallite size is more visible. It decreases from about 58 nm to 35 nm.

Figure 4 shows the temperature characteristics of dielectric constant obtained for discussed ceramics. The broad maximum visible in $\varepsilon(T)$ dependencies in temperature range between 500 K and 530 K is attributed, by other authors, to space charge polarization [21,23,24]. The contribution of polarization of the space charge decreases with temperature.

As the sinter time increases, the discussed maximum increases, reaching the highest value for 12 hours of sintering times (Table 3). Then, the value of maximum is reduced – this behavior can be associated with changes in the concentration of space charge. Above 700 K, the value of dielectric permittiv-

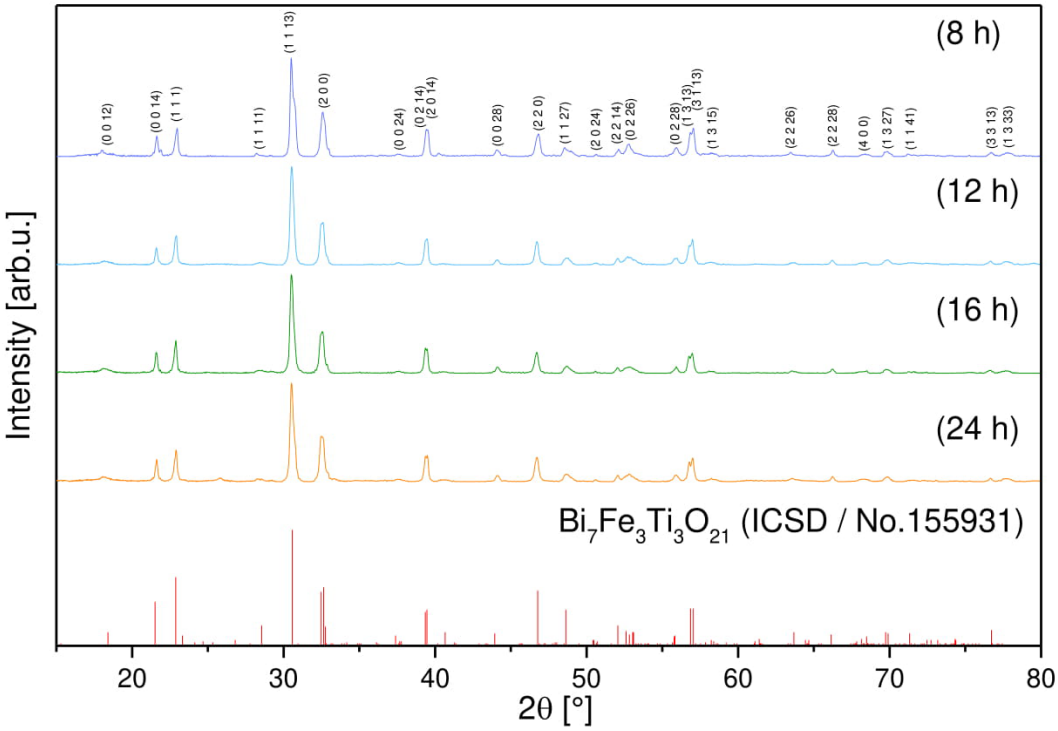

Fig. 3. A set of experimental XRD powder diffraction patterns of obtained $Bi_7Fe_3Ti_3O_{21}$ powders and sintered samples with the reference ICSD pattern

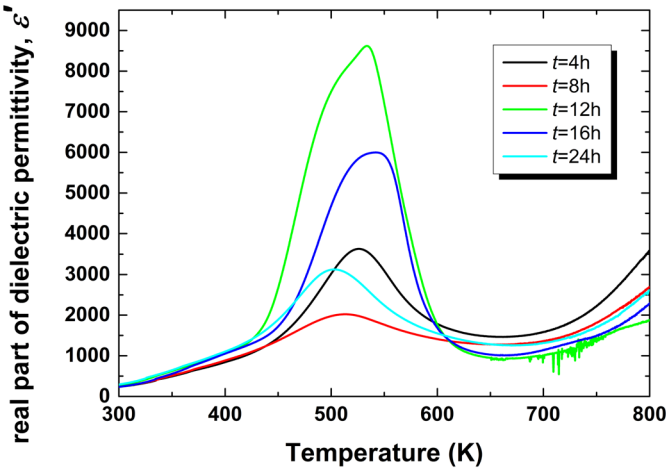

Fig. 4. Temperature characteristics of dielectric permittivity measured on heating at frequency of measuring field 100 kHz for $Bi_7Fe_3Ti_3O_{21}$ ceramics sintered for different time

ity rises again, which is associated with the increasing in high temperature conductivity.

Moreover, the value of dielectric permittivity shows strong frequency dependences, which is particularly visible at the maximum (Figure 5). The degree of dispersion defined as the difference between maximum value of permittivity measured at 0.1 kHz and measured at 1 MHz changed significantly (Table 3).

For low frequencies on presented characteristics in the range of temperature between 600 K and 800 K minimum is visible. The diagram of natural logarithm of the measuring frequency versus the reciprocal temperature T_{min}, at which the minima in the $\varepsilon(T)$ curves occur, is shown in Figure 6.

TABLE 3

Dielectric parameters: dielectric permittivity (ε) and dielectric loss tangent tanδ at room temperature and the maximum value of dielectric permittivity ε_{max} obtained at f = 1 kHz

Sintering time [h]	ε at room temperature (300K)	tanδ at room temperature (300K)	T_{max}	ε_{max}	$\Delta\varepsilon_{max}$
4	234	0.570	526	3630	8933
8	245	0.569	513	2021	15875
12	263	0.625	534	8619	22203
16	235	0.578	542	5997	5427
24	295	0.600	503	3123	12036

Linear character of these dependences proves that the process has activation character and could be described by the following formula :

$$f = f_0 \exp\left(-\frac{E_a}{kT_{min}}\right) \quad (1)$$

The activation energy E_a of the process, which takes place in the sample, was determined by using formula (1). The obtained values are collected in Table 4.

The values of E_a point out that the process is probably connected with the space charge polarization. At low temperature charges are trapped, however the increase in temperature causes gradually release of the space charge. Due to the thermal generation, electrons are released as first. This causes the appearance of nonscreening dipole moments connected with the ions charge. The discussed dipoles give rise to the observed increase of dielectric permittivity in the low frequency range.

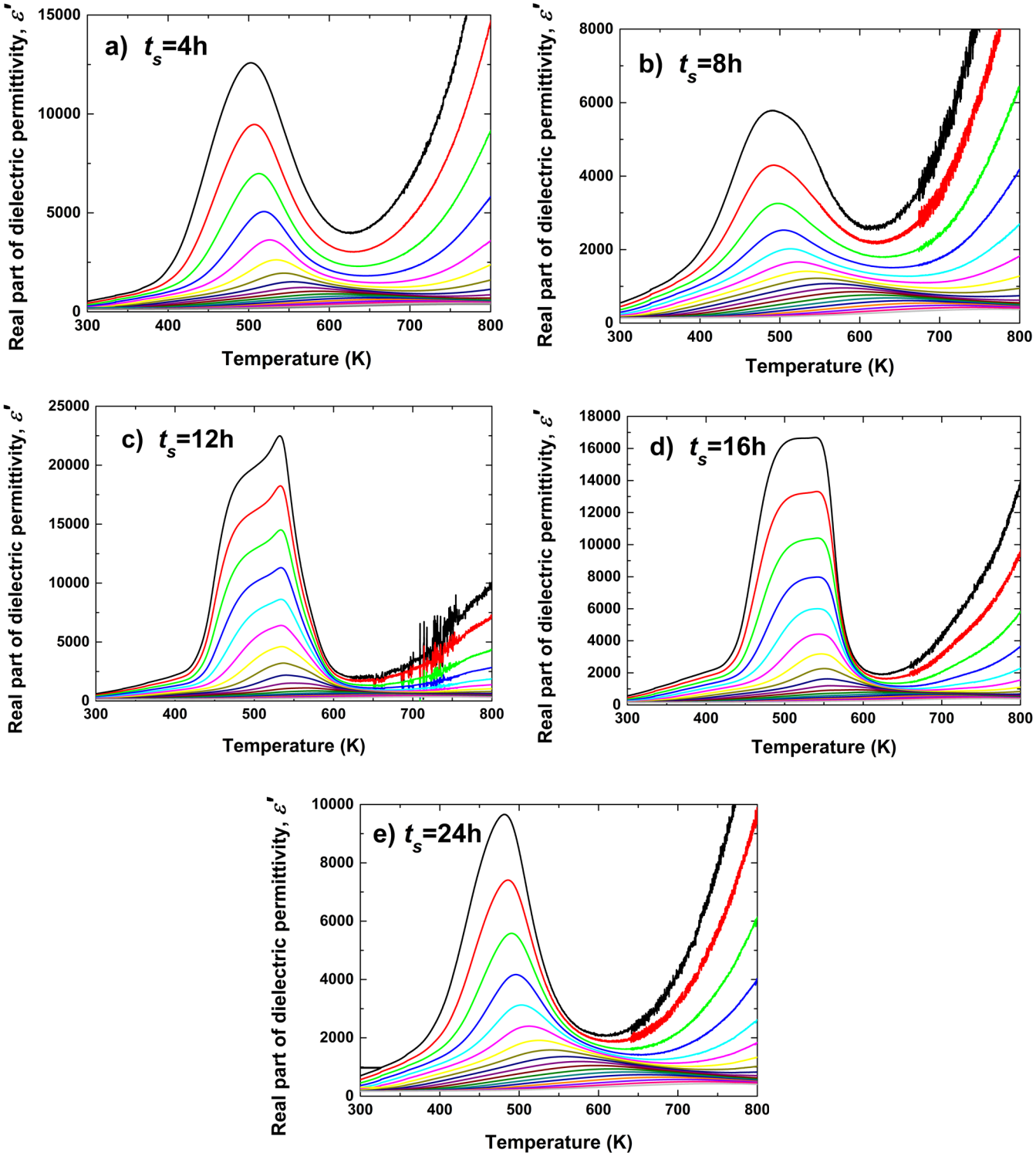

Fig. 5. Real part of dielectric permittivity as a function of temperature for several sintering time a) t_s = 4 h, b) t_s = 8 h, c) t_s = 12 h, d) t_s = 24 h, e) t_s = 24 h

TABLE 4

The activation energy of the process taking place in the samples

Sintering time [h]	E_a [eV]
4	1.12
8	1.21
12	1.30
16	1.71
24	1.12

4. Conclusions

Multiferroic six-layer Aurivillius type $Bi_7Fe_3Ti_3O_{21}$ ceramics was obtained by conventional mixed oxides method. The synthesis took place at the temperature T = 1123 K, and time of it was equal t = 4 h. The conditions of the final sintering proces was carried out at T = 1263 K while the time conditions were change in the range t_s = (4;8;12;16;24) h. The difference

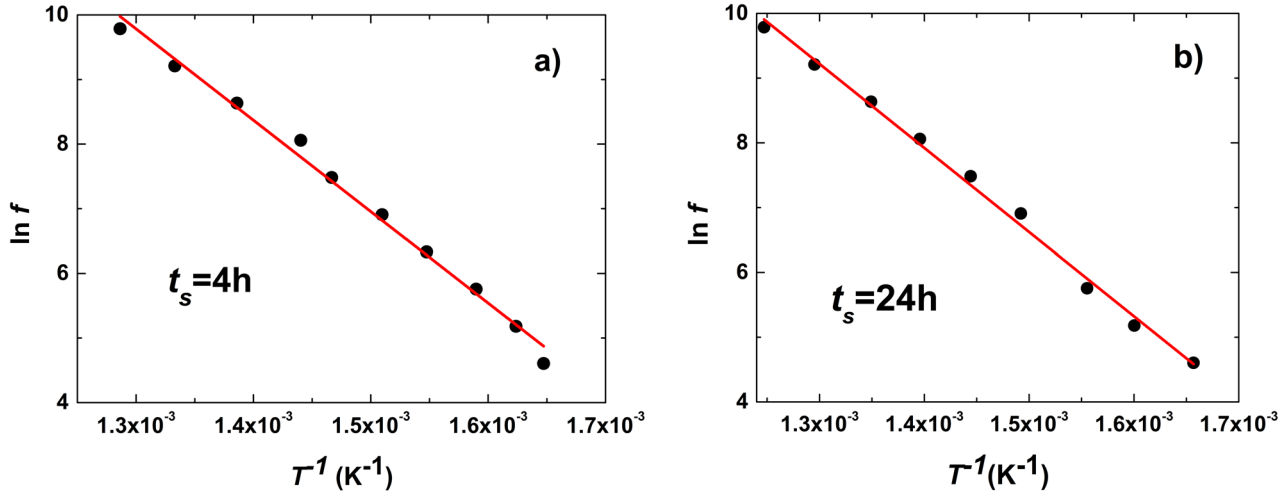

Fig. 6. Natural logarithm of the measuring frequency versus the reciprocal absolute temperatures at which the minima in $\varepsilon(T)$ curves occur a) t_s = 4 h, b) t_s = 24 h

in sintering time determined changes in the microstructure of discussed ceramic materials. Shape of grains drastically changed from platelet-like grains (sintering time t_s = 4 h) to completely different rounded edges shape (longer sintering time). Prolonging the sinter time caused a significant reduction in the size of the crystallites, without significantly affecting the parameters of the unit cell. Dielectric measurements revealed the broad maximum visible in $\varepsilon(T)$ dependencies in the temperature range between 500 K and 530K, which can be connected to the space charge polarization. Additionally in the range of temperature between 600 K-800 K, for low frequencies on $\varepsilon(T)$ characteristic the local minimum is visible, which temperature is strongly dependent on frequency. The process responsible for the behavior has activation characters. The determined activation energy indicated that the process is connected with the relaxation of ions dipoles giving rise to the observed increase of ε in the low frequency range.

Acknowledgement

This work was partially supported by the University grant "New crystalline and composite materials for optics and photonics", UGB 521-9000-00-000, funds for year 2020.

REFERENCES

[1] D.I. Khomskii, J. Magn. Magn. Mater. **306**, 1-8 (2006).
[2] C.A.F. Vaz, U. Staub, J. Mater. Chem. C. **1** (41), 1-29 (2013).
[3] M. Guennou, M. Viret, J. Kreisel, C. R. Phys. **16**, 182-192 (2015).
[4] T. Jardiel, A.C. Caballero, M. Villegas, J. Ceram. Soc. JPN. **116** (4), 511-518 (2008).
[5] Q. Wang, Ch. Wang, J.F. Wang, S. Zhang, Ceram. Int. **42**, 6993-7000 (2016).
[6] K. Zheng, Y. Zhou, L. Gu, X. Mo, G.R. Patzke, G. Chen, Sens. Actuator. **148**,240-246 (2010).
[7] A. Moure, A. Castro, L. Pardo, Prog. Solid State Chem. **37**, 15-39 (2009).
[8] H. Yan, H. Zhang, M.J. Reece, X. Dong, Appl. Phys. Lett. **87**, 082911 (2005)
[9] B. Aurivillius, I. Ark. Kemi. **1** (1), 463-471 (1949).
[10] N.A. Lomanova, M.I. Mozorov, V.L. Ugolkov, V.V. Gusarov, Inorg. Mater. **42** (2), 189-195 (2006).
[11] S.V. Suryanarayana, A. Srinivas, R.S. Singh, R. S. Indo-Russian Workshop on Micromechanical Systems (1999) doi:10.1117/12.369465.
[12] N.A. Lomanova, V.V. Gusarov, Russ. J. Inorg. Chem. **56** (4), 616-620 (2011).
[13] Y. Huang, L. Mi, J. Qin, S. Bi, H.J. Seo, J. Am. Ceram. Soc. (2018) doi:10.1111/jace.16226.
[14] G. Wang, Y. Huang, S. Sun, J. Wang, R. Peng, Y. Lu, J. Am. Ceram. Soc. **99** (4), 1318-1323 (2016).
[15] S. Sun, Ch. Liu, G. Wang, Z. Chen, T. Chen, R. Peng, Y. Lu, J. Am. Ceram. Soc. **99** (9), 3033-3038 (2016).
[16] M. Krzishanovskaya, S. Filatov, V. Gusarov, P. Paufler, R. Bubnova, M. Mozorov, D.C. Meyer, Z. Anorg. Allg. Chem. **631**, 1603-1608 (2005).
[17] P. Scardi, L. Lutterotti, P. Maistrelli, Powder Diffr. **9** (3), 180-186 (1994).
[18] H. Rietveld, J. Appl. Crystallogr. **2** (2), 65-71 (1969).
[19] M. Krzhizhanovskaya, S. Filatov, V. Gusarov, P. Paufler, R. Bubnova, M. Morozov, D.C. Meyer, Z. Anorg. Allg. Chem. **631** (9), 1603-1608 (2005).
[20] A.L. Patterson, Phys. Rev. **56** (10), 978 (1939).
[21] A. Srinivas, M.M. Kumar, S.V. Suryanarayana, T. Bhimasankaram, Mater. Res. Bull. **34** (6), 989-996 (1999).
[22] Z. Lei, Y. Huang, M. Liu, W. Ge, Y. Ling, R. Peng, X. Mao, X. Chen, Y. Lu, J. Alloys Compd. **600**, 168-171 (2014).
[23] R.E. Newnhamm, R.W. Wolfe, J.F. Dorrain, Mater. Res. Bull, **6**, 1029 (1971).
[24] F. Chu, D. Damjanovic, O. Steiner, N. Setter, J. Am. Ceram. Soc. **78**, 3142 (1995).